SIX DAYS THREE CONFERENCES THREE FORUMS ONE EXHIBITION

EuMW 2023
WAVES BEYOND WALLS

EUROPEAN MICROWAVE WEEK

Messe Berlin hub27
BERLIN, GERMANY

17th–22nd SEPTEMBER 2023
www.eumweek.com

IN PERSON EVENT

26TH EDITION OF THE EUMW WEEK

CONFERENCE PROGRAMME

EUROPE'S PREMIER MICROWAVE, RF, WIRELESS AND RADAR EVENT

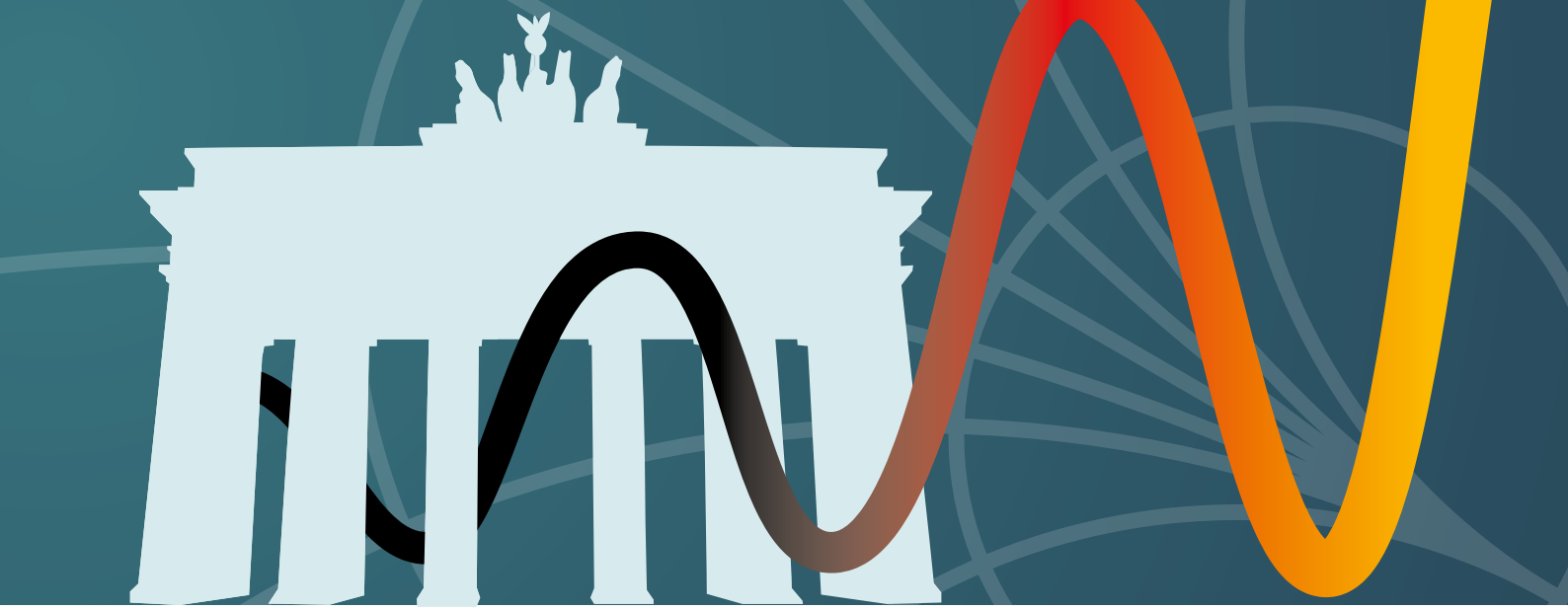

WAVES BEYOND WALLS

Register online at: **www.eumweek.com**

53RD EUROPEAN MICROWAVE CONFERENCE 2023
The 53rd European Microwave Conference

EuMIC 2023
The 18th European Microwave Integrated Circuits Conference

EuRAD 2023
The 20th European Radar Conference

EuMA
European Microwave Association

horizon house

TUESDAY 16:40 – 18:20

ROOM

Beta 8

EuMW05
Special Session APMC

Chair: Wenquan Che[1]

Co-Chair: Maurizio Bozzi[2]

[1]South China University of Technology, [2]University of Pavia

EuMW05-1
Microwave and Millimeter-Wave Filtennas and Their Applications

Xiuyin Zhang[1]

[1]South China University of Technology

EuMW05-2
Recent Progress in Assistant Coil Techniques to Overcome Misalignment Problems in Near-Field Wireless Power Transfer (WPT) Systems

Yongshik Lee[1], SeoYeon Yoon[1]

[1]Yonsei University

EuMW05-3
Theory of Characteristic Modes for Modelling Composite Structures

Chao-Fu Wang[1]

[1]National University of Singapore

Beta 9

EuMC10
New Technologies in Planar Filters

Chair: Giuseppe Macchiarella[1]

Co-Chair: Photos Vryonides[2]

[1]Politecnico di Milano, [2]Frederick Research Center, Cyprus

EuMC10-1
Quasi-Elliptic Multi-Band BPFs Using Multi-Resonant Acoustic-Wave Lumped-Element Resonators

Mohammed R. A. Nasser[1], Dimitra Psychogiou[1]

[1]Tyndall NI/ University College Cork

EuMC10-2
Wideband Reconfigurable Bandpass-to-Bandstop Filter Based on Embedded Switches on Silicon Technology

Miguel Sanchez-Soriano[1], Rozenn Allanic[2], Cédric Quendo[2], Denis Le Berre[2], Douglas Silva De Vasconcellos[3], Virginie Grimal[3], Damien Valente[3], Jérôme Billoué[3]

[1]University of Alicante, [2]University of Brest, [3]University of Tours

EuMC10-3
Compact Dual-band Filters Using Substrate Integrated Coaxial and Slot-line Resonators

Steven Matthew Cheng[1], Dimitra Psychogiou[1]

[1]University College Cork & Tyndall National Institute

EuMC10-4
Quasi-Input Reflectionless Bandpass Filter with Quasi-Elliptic Response and Controllable Transmission Zeros Using Coupled Lines

Girdhari Chaudhary[1], Phanam Pech[1], Samdy Saron[1], Dimitra Psychogiou[2], Yongchae Jeong[1]

[1]Jeonbuk National University, South Korea, [2]University College Cork & Tyndall National Institute

EuMC10-5
Sezawa Mode Enhancement of SAW Resonators on GaN-on-insulator by Optimizing the Metal Thickness and its Application to RF Filters

Yutian Zhang[1], Krishna Balram[1], Martin Cryan[1]

[1]University of Bristol

Quasi-Input Reflectionless Bandpass Filter with Quasi-Elliptic Response and Controllable Transmission Zeros Using Coupled Lines

Girdhari Chaudhary[#], Phanam Pech[#], Samdy Saron[#], Dimitra Psychogiou[*^], Yongchae Jeong[#]

[#]Jeonbuk National University, South Korea

[*]University College Cork, Ireland

[^]Tyndall National Institute, Ireland

girdharic@jbnu.ac.kr, ycjeong@jbnu.ac.kr

***Abstract* — This paper presents a detailed RF design methodology for quasi-elliptic bandpass filter (BPF) with quasi-input reflectionless behaviour in both their passband and stop-band regions. The proposed input reflectionless BPF consists of microstrip coupled lines and transmission lines, comprising three sections: a BPF, a transmission zero (TZ) and an input matching sections. A quasi-elliptic transfer function is achieved by generating TZs at lower and upper sides of passband without affecting the passband response or input reflectionless behaviour. The TZs can be located close to the passband for achieving sharper power absorption ratio profiles within the stopband-to-passband transitions. The theoretical foundation and design methodology of the proposed quasi-elliptic input reflectionless BPF are described. To validate the proof-of-concept, a prototype was manufactured and measured at center frequency of 3.5 GHz. The measured results are fair agreement with the EM simulations and theoretically predicated results.**

***Keywords* — Bandpass filter (BPF), coupled lines, group delay analysis approach, input reflectionless, quasi-elliptic response, transmission zeros (TZs).**

I. INTRODUCTION

Bandpass filters (BPFs) are fundamental component of every RF font-end. Over the last a few decades, various BPF topologies and techniques have been explored. However, conventional BPFs allow transmission signals in passband regions, while signals at stopband regions are reflected back to the source, which can deteriorate the characteristics of other microwave components in RF front-end systems [1]. Therefore, reflectionless filters have a critical importance for enhancing the signal-to-noise ratio (SNR) of their RF front ends as they absorb the incident power in the stopband rather than reflecting it [2], [3]. High frequency selective BPF with as minimum as possible input reflection at passband and stop-band regions are highly demanded for realization of high SNR in RF front ends.

In recent years, several types reflectionless BPF have been explored using different techniques and topologies [4]-[8]. A class of reflectionless filters presented in [4] and [5] by using even-and odd-mode circuit analysis and realized with lumped elements and transmission lines (TLs). Reflectionless filters with matched two ports are reported in [6] by using coupled-ladder filter topologies. Similarly, reflectionless BPF are realized by exploiting two-channel circuit structures, including

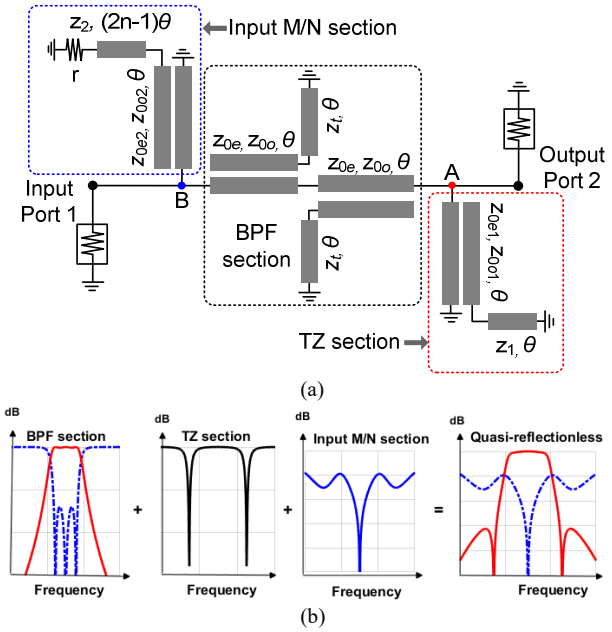

Fig. 1. (a) Circuit schematic of the proposed quasi-elliptic quasi-input reflectionless BPF, and (b) conceptual power transmission and reflection responses of the proposed quasi-input reflectionless BPF.

BPF section and complementary bandstop filter (BSF) section, where non-transmitted out-of-band RF power is dissipated the resistor terminated BSF section [7].

In [8], a rigorous design of an input reflectionless filter with Chebyshev response is presented, however, the frequency selectivity is poor. Despite of significant advances in reflectionless BPF design, a few works have focused on the design of quasi-elliptic input reflectionless BPF as for examples in [9] and [10].

This paper presents a design methodology of quasi-input reflectionless BPF with quasi-elliptic response based on single layer microstrip coupled lines and TLs. The quasi-elliptic response can be achieved by generating two transmission zeros (TZs) very closely to the passband, providing sharper power absorption ratio profiles within the stopband-to-passband transitions. The simple design equations of the BPF are derived using the group delay analysis approach.

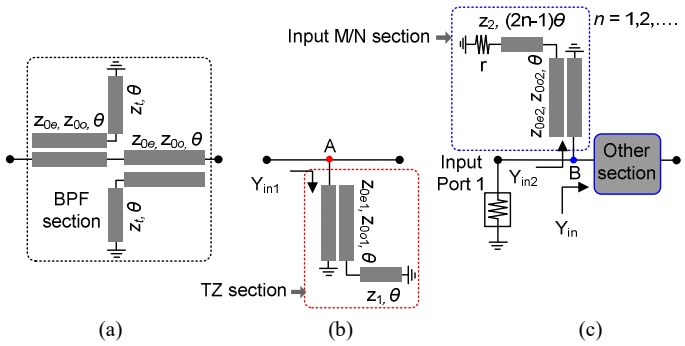

Fig. 2. (a) Proposed 3rd -order coupled line BPF section, (b) TZ section, and (c) input matching (M/N) section.

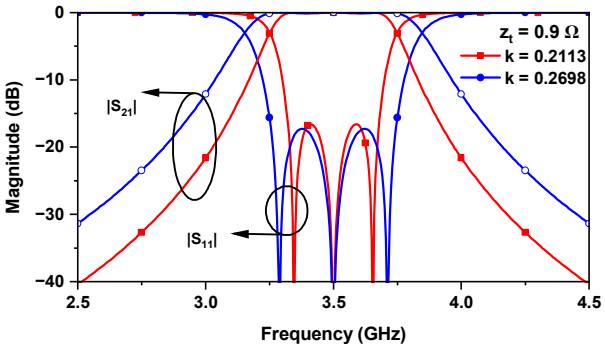

Fig. 3. S-parameters of BPF section results in Fig. (2a) with different coupling coefficient (k) of the coupled lines.

The theoretical foundation and design methodology of the proposed quasi-elliptic input reflectionless BPF are experimentally validated by fabricating a prototype at a center frequency (f_0) of 3.5 GHz.

II. Design Theory

Fig. 1 illustrates the circuit schematic of the proposed quasi-input reflectionless BPF with quasi-elliptic response. It consists of a BPF section, a TZ section, and an input matching (M/N) section. The BPF section is a third order BPF composed of two coupled lines and short-circuited stubs. Similarly, the TZ section comprises a set of coupled lines with a short-circuited TL. The quasi-input reflectionless response is obtained by attaching at the input a set of coupled lines and a resistive terminated TL. For simplicity, all characteristic impedances of coupled lines (z_{0ei}, z_{0oi}) and TLs (z_t, z_1, z_2) are normalized to Z_0 = 50 Ω. The electrical length of coupled lines and TLs are equal to $\theta = \lambda/4$ at f_0.

A. 3rd-order BPF section analysis

Fig. 2(a) illustrates the 3-pole BPF section that uses a coupled line and short-circuited stubs. Conventionally, a parallel coupled line BPF needs N+1 number of coupled lines (N: number of filter stage), which results in a large physical size [11]. However, in this paper, we propose a design of third-order parallel coupled line BPF that utilizes only two coupled lines and short-circuited stubs instead of four (N+1) coupled lines. Assuming that coupling coefficient k_i is a free design variable, z_{0e} is expressed in terms of k and z_{0o} as (1).

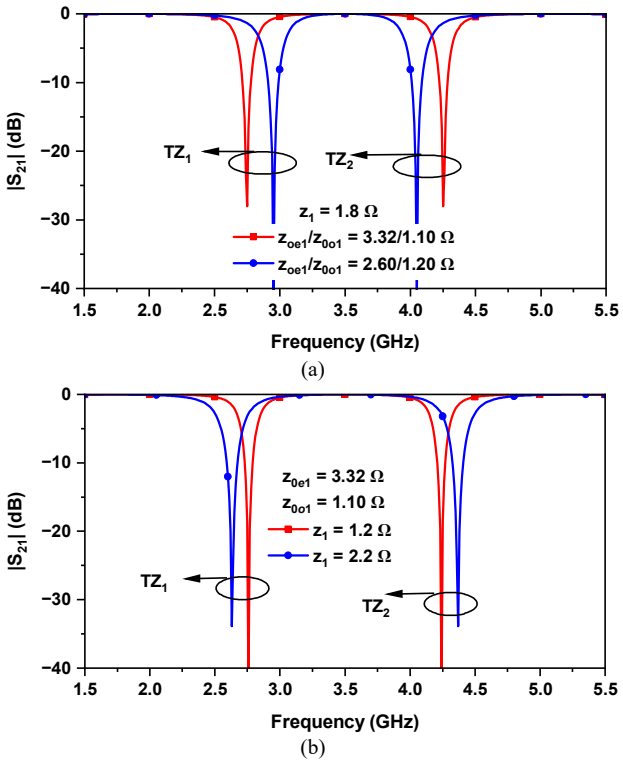

Fig. 4. Transmission zero (TZ) control for different (a) z_{0e1}/z_{0o1} and (b) z_1.

$$z_{0e} = \frac{1+k}{1-k} z_{0o} \tag{1}$$

The group delay (GD) analysis approach has been used to obtain circuit parameters of the proposed BPF section [12]. By equating the GD of the proposed BPF section with that of conventional third-order BPF, the solution of z_{0o} can be found as (2).

$$z_{0o} = \frac{(1-k)\sqrt{z_t^2 + z_t m\left(1 - z_t m k^2\right)} - z_t\left(1-k\right)}{1 - z_t m k^2}, \tag{2}$$

where

$$m = 1 + \frac{2g_1 + g_2}{\pi\Delta} + \frac{(g_1 + 2g_2)\pi\Delta}{4g_1 g_2} \tag{3}$$

and g_i is low-pass prototype element values and Δ is a fractional bandwidth of 3-pole BPF. It should be note that z_{0o} can be obtained by providing the values of k, z_t, and Δ. As this provides a way to design the BPF section with a desired response, the GD analysis can provide an extra degree of freedom that allows for more flexibility in the design of the BPF section compared to conventional parallel coupled BPFs. Once z_{0o} is determined, the value of z_{0e} can be obtained using (1).

For demonstration of the designed equations, Fig. 3 shows the simulated BPF section response with different Δ. In these designs, the low prototype elements are chosen for Chebyshev response with passband ripple of 0.1 dB. As seen from these results, the three-pole BPF response is obtained with two coupled lines and short-circuit stubs. The bandwidth of BPF is controlled by appropriately selecting values of z_t and k of coupled lines. As the coupling coefficient increases, the bandwidth of BPF section increases. The proposed 3-pole BPF

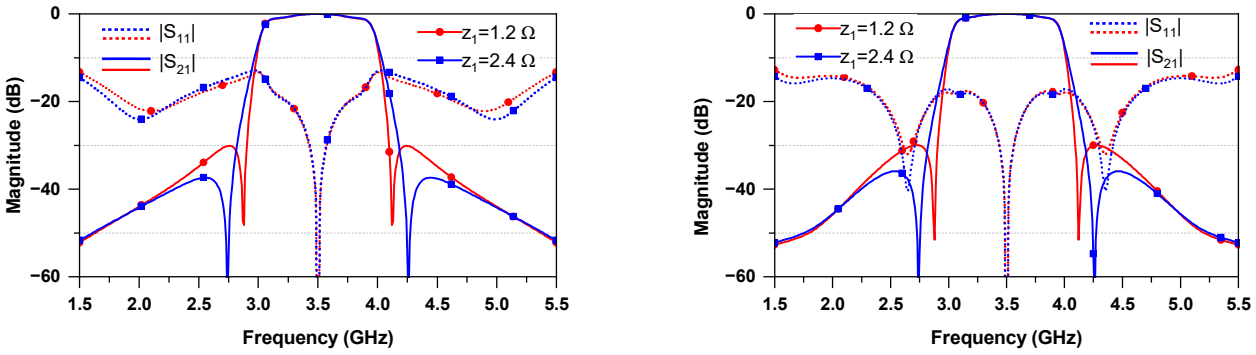

Fig. 5. Simulated S-parameters of the proposed quasi-input reflectionless BPF: (a) the electrical length of matching section TL (n =1) is equal to 90° at f_0 and (b) the electrical length of matching section TL (n =2) is equal to 270° at f_0. Circuit parameters: k = 0.3401, z_{0e} = 2.64 Ω, z_{0o} =1.3 Ω, z_t = 0.6 Ω, z_{0e1} = 3.32 Ω, z_{0o1} =1.2 Ω, z_1 = 1.2/2.4 Ω, z_{0e2} = 2.10 Ω, z_{0o2} = 0.8 Ω, z_2 = 1.8 Ω and r = 1.5 Ω. All circuit parameters are normalized with Z_0 = 50 Ω.

section provides two degrees of freedom to achieve the desired passband response and bandwidth.

B. Transmission zeros and input matching section

Fig. 2(b) shows the TZ section which consists of a coupled line (z_{0e1}, z_{0o1}) and a short-circuited TL with characteristic impedance of z_1 and electrical length θ. The TZ section does not affect the passband of BPF as the input admittance Y_{in1} at point A will be equal to zero at f_0, however, it is infinite ($Z_{in1} = 1/Y_{in1} = 0$) at certain frequencies except f_0. As a result, the TZs are generated at lower and upper sides of f_0. The frequency of TZs can be specified using equation (4).

$$f_{TZ}^{1,2} = \frac{2f_0}{\pi}\cos^{-1}\left\{\pm\sqrt{\frac{z_1\left(z_{0e1}-z_{0o1}\right)^2}{\left(z_{0e1}+z_{0o1}\right)\left(2z_{0e1}z_{0o1}+z_1\left(z_{0e1}+z_{0o1}\right)\right)}}\right\} \quad (4)$$

These TZs improve the selectivity of the proposed input reflectionless BPF without affecting the passband response. Fig. 4 shows the simulated power transmission magnitude of TZ section. As seen from these results, the TZ frequencies at lower and upper stopbands can be controlled by selecting the values of z_{0e1}, z_{0o1}, and z_1 without affecting the passband response.

Fig. 2(c) shows the input matching section, which consists of coupled line (z_{0e2}, z_{0o2}) with electrical length of θ and a resistively-terminated TL with characteristics impedance of z_2 and electrical length of $(2n-1)\theta$ where n is a positive integer value. To achieve input reflectionless response in the proposed structure, input admittance Y_{in2} at point B should be equal to -Y_{in}, where Y_{in} is input admittance at point B looking into the BPF and TZ sections. The value of Y_{in2} is controlled by controlling z_{0e2}, z_{0o2}, and z_2. Therefore, input reflectionless response is achieved by appropriately selecting z_{0e2}, z_{0o2} and z_2.

C. Quasi-input reflectionless BPF with quasi-elliptic response

As described in the previous section, the proposed input reflectionless BPF with quasi-elliptic response is designed by integrating the BPF section, TZ section, and input matching section. For verification purposes, the theoretical power transmission and input reflection responses of designed input reflectionless BPF are shown in Fig. 5.

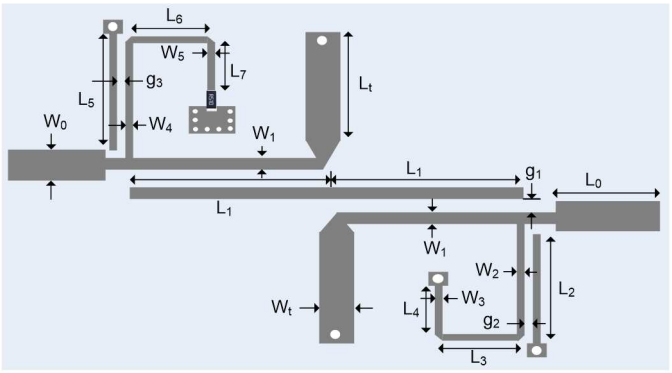

Fig. 6. Physical layout and dimensions of manufactured input reflectionless BPF: W_0 = 2.40, W_1 = W_2 = W_3 = W_4 = W_5 = 0.4, W_t = 2.6, g_1 = 0.2, g_2 = g_3 = 0.22, L_1 = 16, L_2 = L_5 =15.8, L_3 = L_6 = 6, L_4 = 7, L_7 = 5.9, L_0 = 4, L_t = 14, and R = 50 Ω. Dimensions unit: millimeter (mm).

In this example, the electrical lengths of resistor terminated TL are chosen as 90° (n =1 for Fig. 5(a)) and 270° (n = 2 for Fig. 5(b)) for comparison. As shown in these results, a 9-dB input reflection is achieved in both cases (n = 1 and 2) for frequencies extending from 1.5 GHz to 5.5 GHz. The input reflection response of BPF with n = 2 is slightly better than that of BPF with n = 1, but the overall circuit size is larger in case of n = 2. The selectivity in transmission function is achieved by two TZs located at lower and upper sides of passband. In these examples, TZ frequencies are adjusted by controlling z_1 of TZ section while keeping z_{0e1} and z_{0o1} constant. However, it is also possible to control TZ frequencies by controlling z_{0e1} and z_{0o1} of TZ section, while keeping constant z_1. The TZs are moved near passband as z_1 decreases.

III. Experimental Results

For experimental validation, an input reflectionless BPF is designed and manufactured on Taconic substrate with a dielectric constant of 2.2 and thickness of 0.787 mm at f_0 = 3.50 GHz. The goal of the design is to achieve input reflection better than 10 dB at all frequencies and TZ frequencies located at 2.8 GHz and 4.20 GHz.

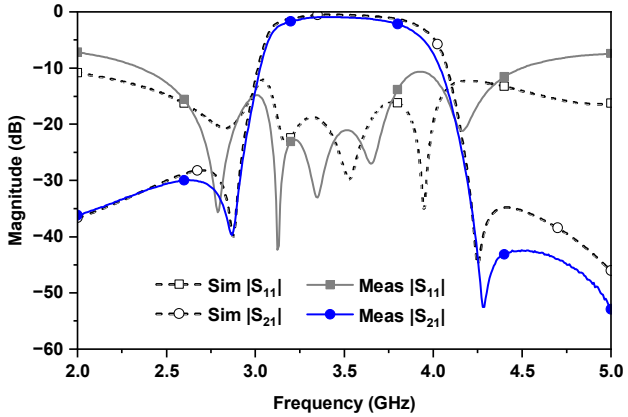

Fig. 7. EM simulated and RF measured S-parameters of the proposed quasi-input reflectionless BPF. Dotted line: simulation and solid line: measurement results.

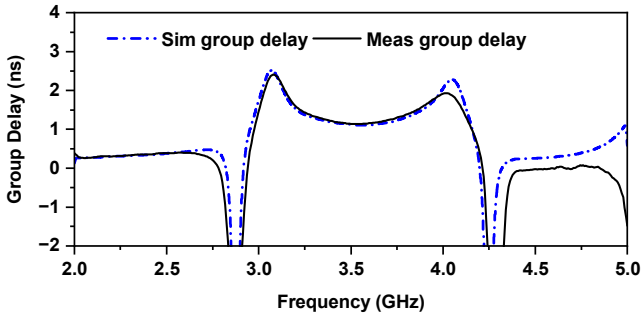

Fig. 8. EM simulated and RF measured group delays of quasi-input reflectionless BPF.

Fig. 6 shows the EM simulation layout of the input reflectionless BPF with its physical dimensions. The simulation was performed using 3-D EM simulator ANSYS HFSS. Fig. 7 shows the comparison between simulated and measured results of the manufactured quasi-input reflectionless BPF. EM simulated input reflection is better than 10 dB for entire passband and stopband regions. The measurement results are consistent with the simulated results, exhibiting a 3-dB bandwidth (BW) of 815 MHz and minimum in-band insertion loss of 0.98 dB, and return loss (RL) > 7.5 dB through its entire passband and stopband regions. The measured input reflection is slightly degraded as compared to EM simulated results due to manufacturing tolerances. Two TZs located at 2.87 GHz and 4.28 GHz provide a quasi-elliptic response and improve selectivity of the proposed input reflectionless BPF. Fig. 8 show the group delay of fabricated filter, while Fig. 9 shows a photograph of manufactured filter.

IV. Conclusion

This paper discusses the RF design of input reflectionless BPF with quasi-elliptic response. The proposed input reflectionless BPF is based on coupled lines and the TZs can be located near the passband by controlling circuit parameters of TZ section without affecting passband response and providing high frequency selectivity characteristics. The design concept of the proposed input reflectionless BPF was experimentally validated at 3.5 GHz through testing filter prototype, which

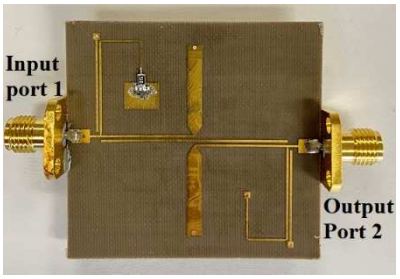

Fig. 9. Photograph of fabricated input reflectionless BPF.

exhibited the following characteristics: input RL > 7.5 dB for all frequencies, minimum IL < 0.98 dB, and two TZs located at near passband.

Acknowledgment

This research was supported by National Research Foundation of Korea (NRF) grant funded by Korea Government (MSIT) (No. RS-2023-00209081) and in part by the Basic Science Research Program through the NRF grant funded by Ministry of Education (No. 2019R1A6A1A09031717).

References

[1] B. Mini-Circuits, "Reflectionless filters improve linearity and dynamic range," *Microwave Journal*, vol. 58, no. 8, pp. 42–50, Aug. 2015.

[2] M. Rais-Zadeh, J. T. Fox, D. D. Wentzloff, and Y. B. Gianchandani, "Reconfigurable radios: A possible solution to reduce entry costs in wireless phones," *Proc. IEEE*, vol. 103, no. 3, pp. 438–451, Mar. 2015.

[3] M. A. Morgan and T. A. Boyd, "Reflectionless filter structures," IEEE *Trans. Microw. Theory Techn*., vol. 63, no. 4, pp. 1263–1271, Apr. 2015.

[4] M. A. Morgan and T. A. Boyd, "Theoretical and experimental study of a new class of reflectionless filter," *IEEE Trans. Microw. Theory Techn.,* vol. 59, no. 5, pp. 1214–1221, May 2011.

[5] J. Lee, B. Lee, S. Nam, and J. Lee, "Rigorous design method for symmetric reflectionless filters with arbitrary prescribed transmission response," *IEEE Trans. Microw. Theory* Techn., vol. 68, no. 6, pp. 2300–2307, Jun. 2020.

[6] A. Guilabert, M. A. Morgan, and T. A. Boyd, "Reflectionless filters for generalized elliptic transmission functions," *IEEE Trans. Circuits Syst. I: Reg. Papers*, vol. 66, no. 12, pp. 4606–4618, Dec. 2019.

[7] R. Gomez-Garcia, J. M. Munoz-Ferreras, and D. Psychogiou, "High-order input-reflectionless bandpass/bandstop filters and multiplexers," *IEEE Trans. Microw. Theory Techn*., vol. 67, no. 9, pp. 3683–3695, Sep. 2019.

[8] J. Lee, J. Lee, and N. S. Barker, "Rigorous design of input-reflectionless filter with Chebyshev response and exact approach to increase reflectionless range," *IEEE Trans. Microw. Theory Techn*., vol. 69, no. 10, pp. 4460-4475, Oct. 2021.

[9] L. Yang, D. Psychogiou, and R. Gomez-Garcia, "Highe-order input-reflectionless quasi-elliptic type wideband bandpass filter using dual-mode stotline resonator," *Proc. Asia Pacific Microw. Conference*, pp. 455-457, 2022.

[10] L. Yang, R. Gomez-Garcia, M. Fan, and R. Zhang "Multilayered input reflectionless quasi-elliptic type wideband bandpass filtering devices on diplexter-based structures," *IEEE Trans. Microw. Theory* Techn., vol. 70, no. 1, pp. 122-138, Jan. 2022.

[11] S. B. Cohn "Parallel-coupled line resonator filters," *IRE Trans. Microwave Theory Techn.*, vol. 6, no. 2, pp. 223-231, Apr. 1958.

[12] J. Lee, G. Chaudhary, P. Phanam, and Y. Jeong, "A design of 3-pole coupled line bandpass filter using group delay analysis approach," *Proc. International Symposium on Antennas and Propagation,* pp. 113-114, Nov., 2022.